Freeform Extrusion of High Solids Loading Ceramic Slurries, Part I: Extrusion Process Modeling

Michael S. Mason[1], Tieshu Huang[2], Robert G. Landers[1],
Ming C. Leu[1], and Gregory E. Hilmas[2]

1870 Miner Circle
Department of Mechanical and Aerospace Engineering[1]
Department of Materials Science and Engineering[2]
University of Missouri - Rolla, Rolla, Missouri 65409–0050
{mmason,hts,landersr,mleu,ghilmas}@umr.edu

Reviewed, accepted September 14, 2006

ABSTRACT

A novel solid freeform fabrication method has been developed for the manufacture of ceramic-based components in an environmentally friendly fashion. The method is based on the extrusion of ceramic slurries using water as the binding media. Aluminum oxide (Al_2O_3) is currently being used as the part material and solids loading as high as 60 vol. % has been achieved. This paper describes a manufacturing machine that has been developed for the extrusion of high solids loading ceramic slurries. A critical component of the machine is the deposition system, which consists of a syringe, a plunger, a ram actuated by a motor that forces the plunger down to extrude material, and a load cell to measure the extrusion force. An empirical, dynamic model of the ceramic extrusion process, where the input is the commanded ram velocity and the output is the extrusion force, is developed. Several experiments are conducted and empirical modeling techniques are utilized to construct the dynamic model. The results demonstrate that the ceramic extrusion process has a very slow dynamic response, as compared to other non-compressible fluids such as water. A substantial amount of variation exists in the ceramic extrusion process, most notably in the transient dynamics, and a constant ram velocity may either produce a relatively constant steady-state extrusion force or it may cause the extrusion force to steadily increase until the ram motor skips. The ceramic extrusion process is also subjected to significant disturbances such as air bubble release, which causes a dramatic decrease in the extrusion force, and nozzle clogging, which causes the extrusion force to slowly increase until the clog is released or the ram motor skips.

1. INTRODUCTION

There have been only a handful of novel SFF systems described in the literature over the past several years [1-7]. Most of these systems have utilized 3D gantry positioning systems. Malone [2] explained that 3D gantries have easy maneuverability and high payload capacities. The emphasis in this work was on high motor accelerations so that a constant deposition feed rate could be utilized. Weiss and Prinz [4] also developed this type of system for customized solid freeform fabrication processes. Some improvements have also been made to the Selective Laser Sintering (SLS) process by reducing the amount of material being heated, thereby improving part accuracy [5-6]. Other areas of improvement have been in Stereolithography by reducing the part shrinkage that is inherent in the process [7]. Freeze-form Extrusion Fabrication (FEF) is a new SFF process that deposits a ceramic slurry utilizing extrusion in a layer-by-layer

fashion to create 3D geometries [8]. The FEF system uses a different approach in mechanical implementation as compared to most other SFF processes. Similar to Rapid Freeze Prototyping [9-12] an XY table with a separate Z elevator axis is used. The 3D gantry and the XY table with Z elevator operate on the same principle. The 3D gantry has all three axes connected into a single unit, which forces the axes to be level with respect to each other, within a specified tolerance, before installation. The XY table and Z elevator are individually known to be level, but the axes must be adjusted to be level relative to each other during installation.

A large amount of ceramic flow modeling research has been conducted. Benbow and Bridgewater developed the standard model for this process [13], which is a static relationship between ram velocity and extrusion force. Other modifications of this model have been developed [14], however this model is still static. A dynamic model of the extrusion process will be developed in this paper to better understand the process.

In the following sections the FEF system will be described in detail, highlighting the major process parameters. The dynamics of the ceramic high solids loading slurry extrusion process will be examined, including system disturbances. In section two each piece of hardware comprising the FEF system is described, as well as its function and interactions with other hardware components. In section three the extrusion process is described. First, the internal system disturbances are discussed along with the effects they have on the extrusion process. Then experimental tests are conducted to characterize the dynamic behavior of the extrusion process.

2. EXPERIMENTAL SETUP

The FEF experimental system (see Figure 1) is composed of three major components: motion system, real-time data acquisition and control system, and extrusion device. Each of the components can be decomposed into several subcomponents, which are described below.

Three Empire Magnetic extended temperature range stepper motors are used to drive Parker Hannifin Daedal 404 XR series linear axes. The three orthogonal linear axes each have 254 *mm* of travel, forming a three-dimensional motion system. The stepper motors have a stepping angle of 1.8 degrees, but have the ability to utilize "micro steps." Micro steps give a motor the ability to take multiple smaller steps to reach a single stepping angle. The stepper motors can vary the micro steps from 1-250 *microsteps/full step* giving a maximum possible resolution of 0.0072 *degrees/step*. The resolution of each axis is 2.5 μm per step, or 0.1 μm per micro-step, when using 250 *microsteps/full step*. The motors have a maximum rotational speed of 50 *rev/s*, which provides a maximum velocity of 250 *mm/s* for the individual axes. The maximum motor angular acceleration is 50 rev/s^2, which provides a maximum linear axis acceleration of 250 mm/s^2.

An extrusion device capable of exerting high pressures is necessary for deposition of high solids loaded ceramics. A stepper motor with a resolution of 16,000 *steps/inch* and maximum velocity of 15 *inches/s* is directly coupled to the Z-axis. The extrusion axis, having eight inches of stroke is used to move a plunging device, which applies pressure to a syringe to extrude ceramic material. The deposition rate can be changed online by adjusting the commanded stepper motor speed. A 60 cm^3 syringe is used to hold and eject the deposition material. Nozzles of diameters ranging from 190 – 580 μm are attached to the end of the syringe to allow for different thicknesses of material to be deposited.

A LC-305 load cell from Omega Engineering is utilized for extrusion force feedback. The load cell measures the force the ram extruder applies to the ceramic slurry. The load cell outputs a differential voltage (0 – 20 *mV*) that corresponds to the extruded force (0 – 4450 *N*). This signal is sent to an amplifier that increases the differential voltage by a factor of 100, thus, the output range is 0 – 2 *V*. This increases the input range, thereby increasing the overall resolution of the feedback device. The load cell has a 0.1% linearity, which gives an output within +/- 4.45 *N* of the actual force.

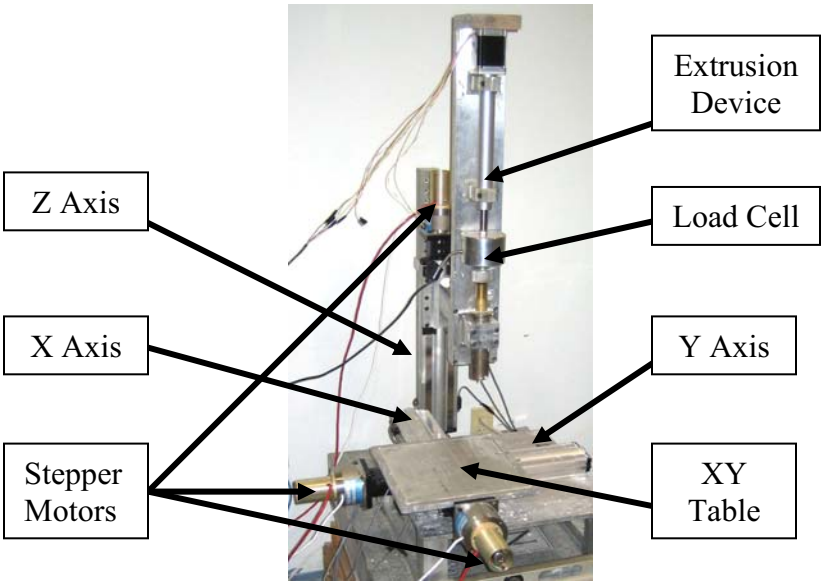

Figure 1: The FEF experimental system.

3. FLOWRATE MODELING

In modeling and controlling the ceramic slurry extrusion process, one must consider the system disturbances and material flow dynamics. The first subsection below describes in detail the two major disturbances that are present within the extrusion process: agglomerate breakdown and air bubble release. The next subsection explains the different types of material flowrate tests conducted in order to characterize the dynamic extrusion process.

3.1 System Disturbances

There are two major disturbances that occur during the extrusion process: agglomerate breakdown and air bubble release. Both of these disturbances cause changes to the ceramic slurry flowrate. The following sections explain why the disturbances are present and how they affect the extrusion process.

3.1.1 Agglomerate Breakdown Ceramic slurries are fluids with significant solids loading. In the case of the FEF process, the solids loading is higher, generally greater than 50 vol. %. The solid particles that are present within the slurry are referred to as agglomerates. When batching the ceramic slurry the ceramic powder is mixed with an aqueous media. The current ceramic of interest is alumina (Al_2O_3), in combination with water as the binding media, Polyethelene-Glycol for improved green part strength, and Aquazol for material lubrication. The materials are mixed

for a period of time to form an isotropic slurry. The ceramic particle size is reduced as much as possible, generally ranging from 0.8 to 2.5 μm. With particles of varying size it becomes increasingly difficult for the particles to be evenly interspersed within the aqueous media. The ceramic particles join together into larger particles called agglomerates. The agglomerates are interspersed within the aqueous media, thereby forming the ceramic slurry.

As force is applied to the ceramic slurry, the material reservoir compresses due to the presence of air bubbles (described later), and material flowrate increases with the rising force. After compression is complete the material flowrate reaches a stable state. As the material enters the nozzle, the space available for agglomerates to be interspersed is significantly reduced. This causes an increase in resistance force for compression of the slurry since the agglomerates are pressed together. After a critical force is reached the agglomerates "slide" across edges of other agglomerates. During the sliding process the agglomerates break into smaller agglomerates allowing for material flow to continue. Figure 2 shows an example of agglomerate breakdown.

The force spikes caused by agglomerate breakdown cannot be reliably predicted. The agglomerate size is random and is different for each slurry preparation. The breakdown of the agglomerates also occurs randomly, but can be reduced by minimizing the ceramic particle size.

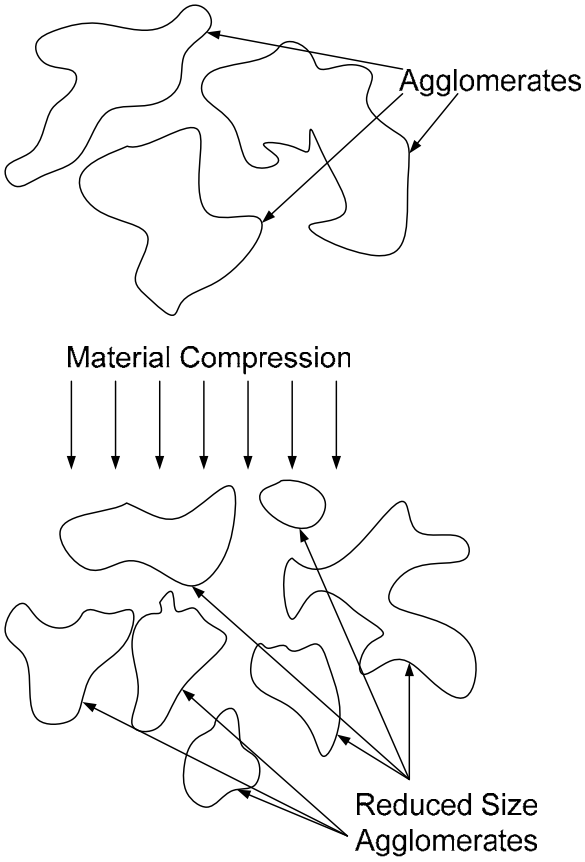

Figure 2: Illustration of agglomerate breakdown.

3.1.2 Entrapped Air Bubble Release During the preparation phase of the ceramic slurry, the slurry is mixed in a vacuum to remove air present within the slurry for a more consistent fluid. After the slurry is mixed, it must be loaded into the fluid reservoir. Due to the high solids loading the fluid is extremely viscous and requires manual loading into the syringe. During the

loading process air becomes entrapped, forming bubbles within the ceramic slurry. As the ram applies force to the ceramic slurry, the air bubbles compress due to buoyancy effects from the surrounding slurry. As material is extruded the air bubbles are forced into the die region (see Figure 3), which is much smaller than the rest of the syringe. The air bubbles join together as they enter the die region, forming larger bubbles (Figure 4). As the air bubbles reach the nozzle exit they pop, creating a large pressure release. This causes the extrusion force to dramatically drop. The region previously occupied by the air bubble is now empty allowing for the ceramic slurry to expand.

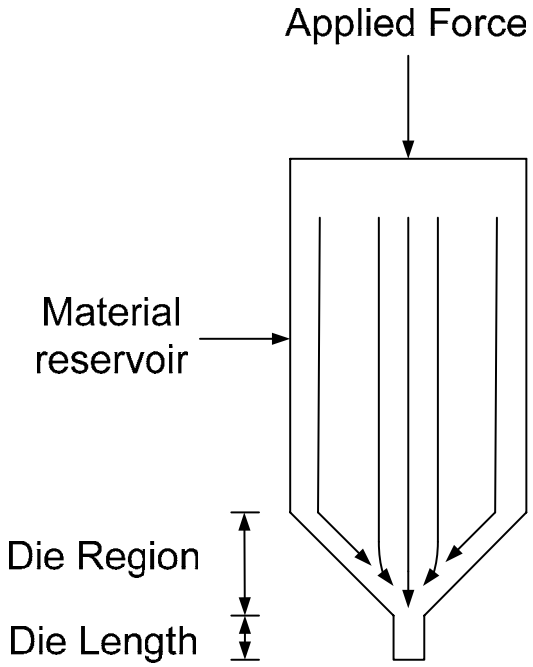

Figure 3: Illustration of slurry flow within material reservoir.

3.2 Flowrate Tests

For modeling the ram extrusion process two different types of tests were conducted. It was first necessary to determine the ram velocity operational range. This was determined by running the ram extrusion velocity at various speeds and visually inspecting the extrudate for curling and clogging. Curling is the phenomenon where the extrudate curls on the nozzle tip, as shown in Figure 5. Clogging is when extrudate dries within the nozzle and reduces the material flowrate until no material can be extruded through the nozzle. Neither of these situations are desirable. The extrusion velocity range for the ceramic slurries in this paper was determined to be 0.2 to 0.65 $\mu m/s$. Velocities below the lower range lead to clogging, while velocities above the higher range cause curling, which will eventually lead to clogging. It should be noted that velocities outside the operational range can be used, but only for short periods of time.

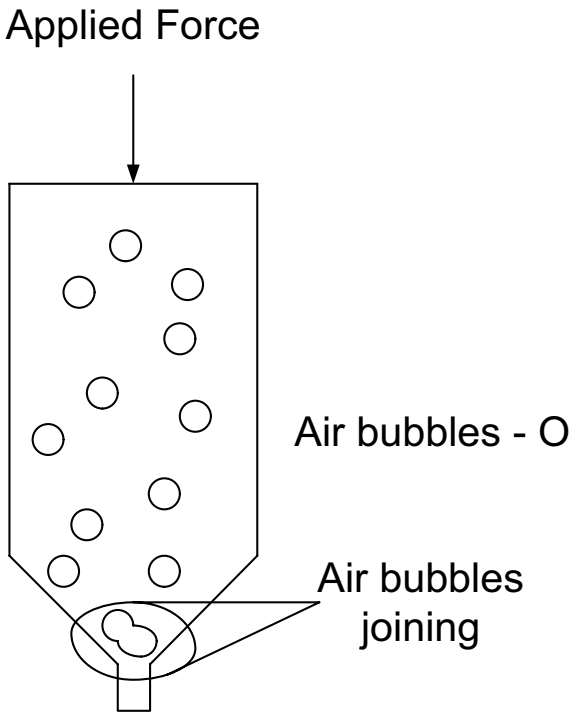

Figure 4: Illustration of entrapped air bubbles within material reservoir.

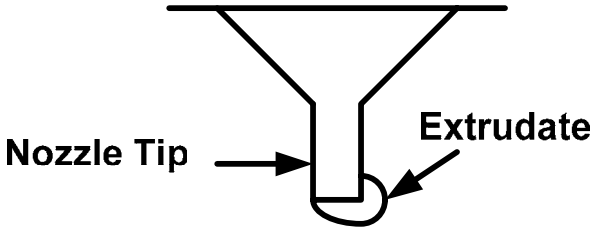

Figure 5: Curling of extrudate on nozzle tip.

3.2.1 Long-Step Tests A series of step tests with constant ram velocities were conducted. The commanded ram velocity was kept constant for one hour and extrusion force and mass data were collected at a rate of 1 *Hz*. The mass data was collected through a mass balance connected to the PC through a USB port. The mass balance was set to a baud rate of 9200 and continuous acquisition. A total of seven tests were conducted at different velocities within the range of interest using a 190 μm diameter nozzle. During most of the tests the extrusion force rose exponentially during the transient phase and a relatively constant force was reached in the steady state. However, in some tests the force continued to rise at a slow rate during the entire test, never reaching a relatively constant force.

Empirical modeling was performed to determine a model for each test conducted. A first-order model of the form

$$\frac{F(s)}{v(s)} = \frac{K}{\tau s + 1} \tag{1}$$

where K is the gain and τ is the time constant. This model was fit to each set of experimental data. To find the steady-state extrusion force an average was taken over the region following the

initial force rise. The time constant varied for each of the extrusion velocities, but each was found to be at a minimum 200 *s*. Table 1 shows the ram velocity, time constant, gain, and steady state extrusion force for each test. Figures 6-8 show some of the test and model results. Figures 7 and 8 show that the process may not be repeatable. For the same velocity input, test 2 reached a steady-state extrusion force in approximately 15 *min*; however, during test 3 the extrusion force increased during the entire testing period (i.e., 60 *min*). Test 3 had an initial extrusion force of approximately 50 *N*, which is different from test 2, but this should not cause the extrusion force to reach a steady-state value more slowly. Tests 3 and 9 did not reach steady state during the one-hour period and were therefore not included in the linear relationships found.

Table 1: Data for constant velocity step tests.

Test (#)	v (μm/s)	τ (sec)	K (N/μm/s)	F_{ss} (N)	m (mg/s)
1	0.3	200	433	130	29.9
2	0.4	200	450	180	36.1
3	0.4	----------	----------	----------	----------
4	0.45	500	467	210	36.8
5	0.45	600	644	290	46.1
6	0.5	250	500	250	45.0
7	0.55	900	564	310	50.0
8	0.6	225	533	320	55.0
9	0.6	----------	----------	----------	----------
	Average	319	513		
	σ	268	74		

The large time constants demonstrate that the ceramic slurry extrusion process is extremely slow as compared to other incompressible fluid flow systems such as water where the time constant is on the order of 10 *ms* [15]. The larger response time may be due to the viscosity characteristics of the ceramic slurry. If the slurry is a non-Newtonian fluid, then the viscosity increases with increasing fluid shear rate, which is directly affected by the ram velocity. Future work will need to be conducted to investigate this hypothesis.

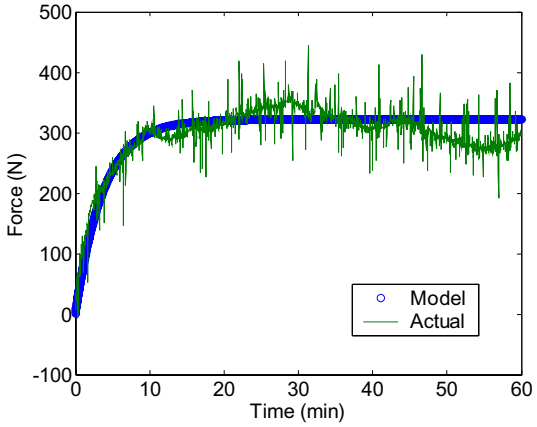

Figure 6: Constant velocity test (#8) with ram extrusion $v = 0.6$ *μm/s* and $F_{ss} = 320$ *N*.

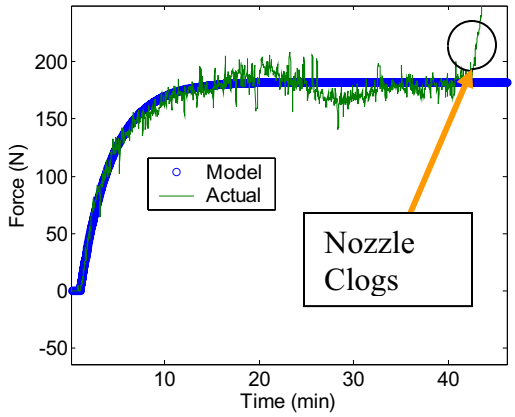

Figure 7: Constant velocity test (#2) with ram extrusion $v = 0.4$ $\mu m/s$ and $F_{ss} = 180$ N.

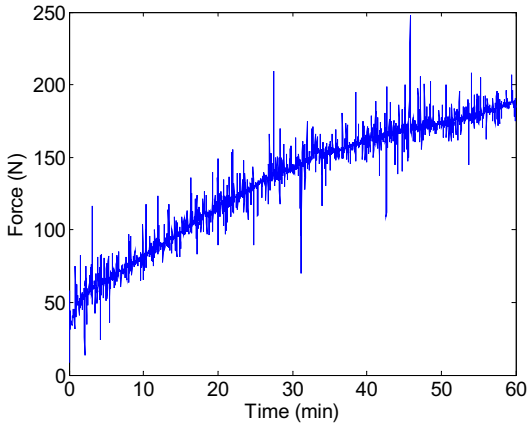

Figure 8: Constant velocity test (#3) with ram extrusion $v = 0.4$ $\mu m/s$.

Least squares was utilized to relate the three parameters, steady state extrusion force, ram velocity, and mass flowrate, to each other. Three relationships were considered: mass flowrate versus extrusion force, mass flowrate versus ram velocity, and extrusion force versus ram velocity. Equations (2)-(3) show the relationships between the three parameters (mass flowrate, extrusion force, and ram velocity) and Figures 9 and 10 show the test data with the linear relationships. Even though the y intercept values were determined there is no physical meaning to them because equations (2)–(3) are only valid for ram velocities in the range of 0.3-0.6 $\mu m/s$. The Δ's in (2)-(3) refer to the changes between the parameters in relation to each other over the given range of ram velocity values.

$$\frac{\Delta m_{ss}}{\Delta F_{ss}} = 0.70 \tag{2}$$

$$\frac{\Delta m_{ss}}{\Delta v_{ss}} = 50 \tag{3}$$

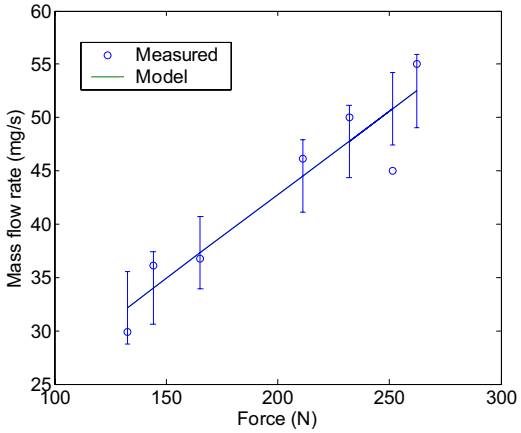

Figure 9: Steady-state mass flowrate versus steady-state extrusion force. Error bars correspond to one standard deviation.

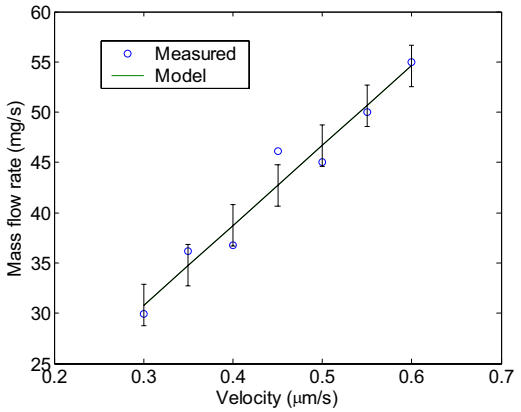

Figure 10: Steady-state mass flowrate versus steady-state ram velocity. Error bars correspond to one standard deviation.

One standard deviation of the curve fit is shown by the error bars in Figures 9-10. The standard deviations are 3.4 *mg/s* and 2.1 *mg/s* for equations (2)-(3), respectively. As can be seen from the figures, there is a definite correlation relating the three parameters. The correlation coefficients for mass flowrate to extrusion force, mass flowrate to ram velocity, and extrusion force to velocity are 0.9356 and 0.9764 respectively.

3.2.2 Short-Step Test The next test conducted was a short step test in which the ram extruder ran at velocities covering the range of interest. The velocities incremented and decremented by 0.05 *μm/s* every 40 seconds. The initial velocity was run for a period of 8 *min*, which was determined to be the average time for a given ram velocity to reach a steady-state extrusion force, in order for the extrusion force to be constant before the test was started. The time history of the commanded velocity and corresponding extrusion force are shown in Figure 11. Force data was collected at a rate of 20 *Hz*.

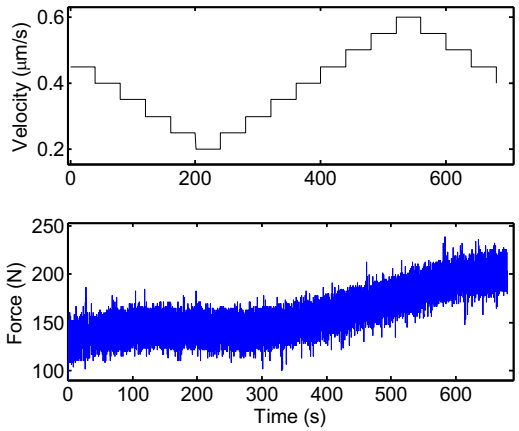

Figure 11: Ram velocity and extrusion force time history for short step test.

As discussed before, the extrusion force increases with an increase in ram velocity. After examining the extrusion force data it can be seen there is a delayed reaction between the change in ram velocity and the change in the extrusion force. The ram velocity decreases by 0.05 *μm/s* for the first 5 time periods, but the extrusion force does not start to decrease until 200 *sec*, at which point the ram velocity has dropped to 0.2 *μm/s*. At 240 *sec* the ram velocity is increased to 0.25 *μm/s*, but the extrusion force continues to decrease until 280 *sec*. At this time the ram velocity is 0.3 *μm/s*. The ram velocity continues to increase up to 0.6 *μm/s* at 520 *sec* while the extrusion force keeps increasing until 640 *sec*, two time periods after the ram velocity has been decreased. During the remaining time the extrusion force is constant. Another interesting trend that can be seen in Figure 11 is that the extrusion force increases at a faster rate with increasing ram velocity than it decreases with decreasing ram velocity. This is believed to be due to material compression effects. The ceramic slurry is a solid/liquid mixture. Both of these are considered incompressible material states, but with the presence of agglomerates and air bubbles within the material reservoir a small amount of compression is possible. As previously mentioned the agglomerates can breakdown which allows for compression as well as the air bubbles present. As material within the reservoir reduces, the amount of compression possible decreases due to the extrusion of air bubbles and the breakdown of agglomerates to a relatively small size.

Another type of short-step test consisted of applying a constant ram velocity for a fixed period of time and then reducing the ram velocity for the same period of time. This ram velocity cycle is repeated for the entire test.

Two different types of impact tests were conducted. Extrusion force data was collected at a rate of 10 *Hz*. The first test conducted had lower ram velocities of 0.5 *μm/s* and higher ram velocities that started at 5 *μm/s* and increased by 5 *μm/s* every other time period. Figure 12 shows the results. As can be seen the higher the ram velocity the faster the extrusion force increased. Also, there is a delayed reaction between the change in ram velocity and change in extrusion force, which ranges from 0-9 *sec*. It can be seen that the extrusion force increased so fast the ram motor eventually skipped.

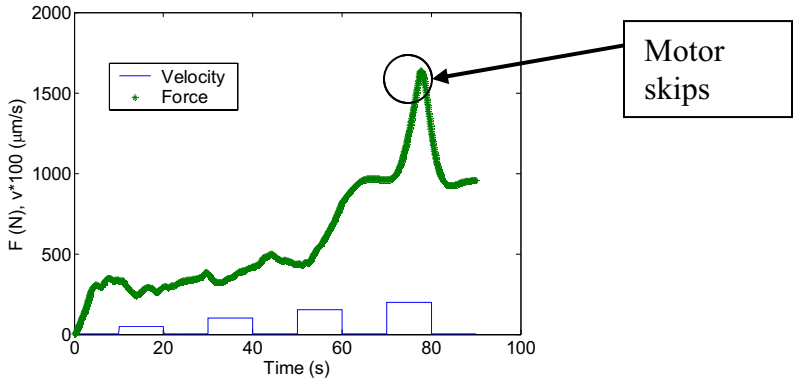

Figure 12: Impact test with increasing ram velocities.

The second test conducted repeatedly changed the ram velocity between 0.5 and 5 *μm/s* every 40 *sec*. The application periods were too long, thereby causing the motor to skip as shown in Figure 13. The time period was then reduced to 10 *sec* for the last two test runs. Figure 14 shows more clearly the effect the value of the extrusion force has on the rate at which the extrusion force increases and decreases. The 0-9 *sec* delay is present for every change in ram velocity input. With a total of 73 individual ram velocity changes it was visually examined that the delay for increasing ram velocity was higher than for decreasing ram velocity. The average delay for increasing ram velocity was 4.3 *sec* with a standard deviation of 1.31 *sec* as calculated from 37 ram velocity increases. The average delay for decreasing ram velocity was 2.5 *sec* with a standard deviation of 1.5 *sec* calculated from 36 ram velocity decreases.

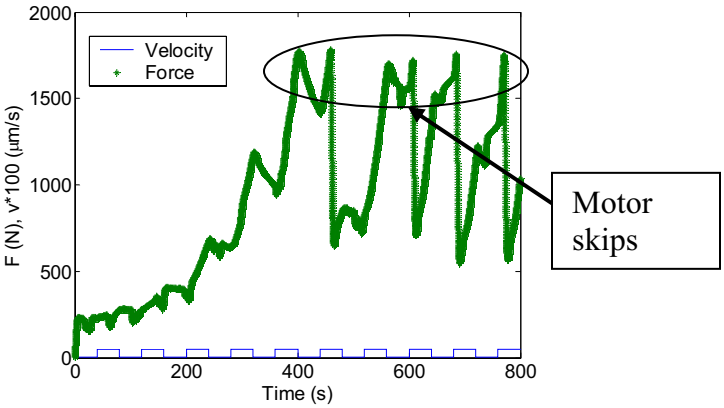

Figure 13: Repeated ram velocity inputs for 40 *s* periods.

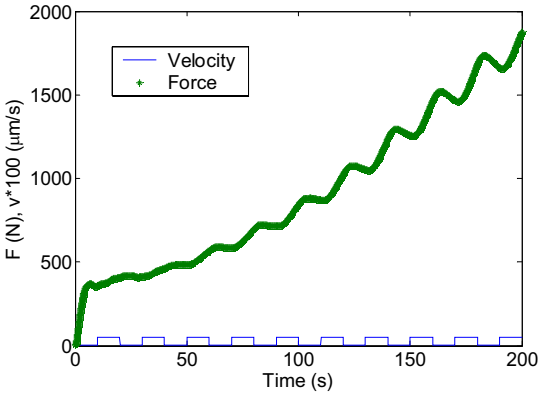

Figure 14: Repeated ram velocity inputs for 10 *s* periods.

4. SUMMARY AND CONCLUSIONS

A new environmentally friendly solid freeform fabrication technique, Freeze-form Extrusion Fabrication (FEF), has been developed utilizing aqueous ceramic slurries as the build material. The FEF system was described in detail highlighting the major hardware components. System disturbances were described along with their effects on material flowrate behavior. Multiple tests were conducted in order to characterize the dynamics of the ceramic slurry utilizing a ram extruder. A first-order process model was developed and compared to collected data.

From the large time constant values obtained from the extrusion tests conducted it was shown that the slurry flowrate is much slower when compared to other incompressible fluid flows such as water. There is a large variability in the value of the time constant, indicating that the process is not very repeatable. The ram velocity, extrusion force, and mass flowrate have also been shown to be highly correlated from the long-step tests conducted with correlation coefficients of 0.93 or higher. From the short-step tests it was shown that there are likely to be different dynamics present between increasing and decreasing extrusion force because there is a faster increase in extrusion force from higher ram velocities than a decrease in extrusion force due to a reduction in ram velocity.

ACKNOWLEDGEMENTS

This work was supported by the Air Force Research Laboratory under Contract FA8650-04-C-5704. The authors would also like to thank Mike Hayes of Boeing for his technical support and Justin Kayser for his time and effort in this research project.

REFERENCES

1. K. Taminger, R. Hafley, D. Fahringer, and E. Martin, “Effect of Surface Treatments on Electron Beam Freeform Fabricated Aluminum Structures,” Langley Technical Reports (2004).
2. E. Malone, R. Rasa, D. Cohen, T. Isaacson, H. Lashley, and H. Lipson, “Freeform Fabrication of 3D Zinc-Air Batteries and Functional Electro-Mechanical Assemblies,” *Rapid Prototyping Journal*, Vol. 10, No. 1, 58-69 (2004).
3. H. Lipson and J.B. Pollack, “Automatic Design and Manufacture of Artificial Lifeforms,” *Nature*, Vol. 406, 974-978 (2000).

4. L. Weiss and F. Prinz, "Novel Applications and Implementations of Shape Deposition Manufacturing," Naval Research Reviews, Vol. 1, Office of Naval Research (1998).
5. H. Gothait, Object Geometries, Patent 6850334 (2000).
6. B. Jang, J. Duan, K. Chen, and E. Ma, Nanotek Instruments Inc., Patent 6405095 (2002).
7. M. Guertin, C. Hull, and H. Nguyen, 3D Systems, Patent 6399010 (2002).
8. T. Huang, M. Mason, G. Hilmas, and M. C. Leu, "Freeze-form Extrusion Fabrication of Ceramics," *Proceedings of Solid Freeform Fabrication Symposium*, August 1-3, Austin, Texas, 72-85 (2005).
9. G. Sui, "Modeling and Analysis of Rapid Freeze Prototyping," PhD Dissertation, University of Missouri-Rolla, Rolla, Missouri (2002).
10. F. Bryant, G. Sui, and M. C. Leu, "A Study on the Effects of Process Parameters in Rapid Freeze Prototyping," *Proceedings of Solid Freeform Fabrication Symposium*, August 5-7, Austin, Texas, 635-642 (2002).
11. M. C. Leu, W. Zhang, and G. Sui, "An Experimental and Analytical Study of Ice Part Fabrication with Rapid Freeze Prototyping," *Annals of the CIRP*, Vol. 49/1, 147-150 (2000).
12. G. Sui, and M. C. Leu, "Investigation of Layer Thickness and Surface Roughness in Rapid Freeze Prototyping," *ASME Journal of Manufacturing Science Engineering*, Vol. 125/3, 555-563 (2002).
13. J. Benbow and J. Bridgwater, *Paste Flow and Extrusion, Oxford Series on Advanced Manufacturing*, Vol. 10, Clarendon Press, Oxford (1993).
14. P. Martin, D. Wilson, and K. Challis, "Extrusion of Paste Through Non-Axisymetric Systems" *6*th *World Congress of Chemical Engineering,* Melbourne, Australia, September 23-27 (2001).
15. M. Munson, D. Young, and T. Okiishi, *Fundamentals of Fluid Mechanics*, Third Edition, New York, John Wiley and Sons Inc., 462-468 (1998).